Histochem Cell Biol (2002) 118:41–49
DOI 10.1007/s00418-002-0425-z

ORIGINAL PAPER

Christine Gersch · Oliver Dewald · Martin Zoerlein
Lloyd H. Michael · Mark L. Entman
Nikolaos G. Frangogiannis

Mast cells and macrophages in normal C57/BL/6 mice

Accepted: 17 May 2002 / Published online: 18 June 2002

Abstract Mast cells and macrophages have an important role in immunity and inflammation. Because mice are used extensively for experimental studies investigating immunological and inflammatory responses, we examined mast cell and macrophage distribution in normal murine tissues. Mast cells were abundant in the murine dermis, tongue, and skeletal muscle but were rarely found in the heart, lung, spleen, kidney, liver, and the bowel mucosa. In contrast, dogs exhibited large numbers of mast cells in the lung parenchyma, liver, and bowel. Some murine dermal mast cells had long cytoplasmic projections filled with granular content. Mouse mast cells demonstrated intense histamine immunoreactivity and were identified with histochemical enzymatic techniques for tryptase and chymase. Macrophages, identified using the monoclonal antibody F4/80, were abundant in the spleen, lung, liver, kidney, and bowel but relatively rare in the heart, tongue, and dermis. Using a nuclease protection assay we investigated mRNA expression of stem cell factor (SCF), a crucial survival factor for mast cells, and the macrophage growth factors macrophage colony stimulating factor (M-CSF) and granulocyte macrophage colony stimulating factor (GM-CSF). Stem cell factor mRNA was highly expressed in the murine lung. Relatively low levels of SCF mRNA expression were found in the tongue and earlobe, which are tissues containing a high number of mast cells. Macrophage CSF and GM-CSF mRNA was highly expressed in the lung and spleen. The murine heart, an organ with a low macrophage content, expressed high levels of M-CSF but negligible levels of GM-CSF mRNA. Constitutive growth factor mRNA expression in murine tissues without significant populations of mast cells and macrophages may suggest an alternative role for these factors in tissue homeostasis.

Keywords Mast cell · Macrophage · Mouse · Tryptase · Growth factors

C. Gersch · O. Dewald · M. Zoerlein · L.H. Michael
M.L. Entman · N.G. Frangogiannis (✉)
Section of Cardiovascular Sciences, Baylor College of Medicine,
One Baylor Plaza M/S F-602, Houston TX 77030, USA
e-mail: ngf@bcm.tmc.edu
Tel.: +1-713-7984188

C. Gersch · O. Dewald · M. Zoerlein · L.H. Michael
M.L. Entman · N.G. Frangogiannis
Department of Medicine the Methodist Hospital
and the DeBakey Heart Center, Baylor College of Medicine,
Houston TX 77030, USA

Introduction

Mast cells and macrophages are important effector cells with an established role in inflammation and immunity. They are capable of producing proteolytic enzymes and a wide variety of cytokines and growth factors (Gordon and Galli 1990; Gordon et al. 1990; Walsh et al. 1991) that may serve as key regulators of the inflammatory process and tissue repair. Both mast cells and macrophages are constitutively present in many normal tissues and organs (Kube et al. 1998; Frangogiannis et al. 1999), especially in locations interfacing with the external environment. Resident macrophages in the spleen, lung, liver, and lymph nodes have an established role in phagocytosis and the immune response, however the role of resident mast cells is less well understood.

The availability of transgenic animals has increased the importance of murine studies in investigating biological processes (Shapiro 1997). Numerous studies have examined the inflammatory response using transgenic and knockout animals in a wide variety of disease models (Kupper 1996; Kanwar et al. 1998; Gu et al. 2000). However, the significant interspecies differences in structure and cellular composition of normal mammalian tissues are rarely recognized (Weindruch and Masoro 1991; Borisov 1999), potentially leading to conclusions that may be of limited usefulness in our understanding of human disease. In addition, significant differences have been reported between various murine strains and may affect the regulation of the inflammatory process (Ghildyal et al. 1994; Rohan et al. 2000). C57/BL/6 mice

have been commonly used as an investigational tool in examining the inflammatory cascade (Fritz and Zhao 2001; Kahn et al. 2001). In this study, we sought to describe in detail the distribution and morphological characteristics of mast cells and macrophages in C57/BL/6 mice. In addition, we examined the expression of stem cell factor (SCF), a crucial factor for the survival and growth of mast cells (Galli et al. 1993, 1994; Smith et al. 2001), and of macrophage colony stimulating factor (M-CSF) and granulocyte macrophage colony stimulating factor (GM-CSF), important factors regulating macrophage growth (Wiktor-Jedrzejczak and Gordon 1996), in normal murine tissues.

Materials and methods

Animal protocols

Eleven normal 8- to 12-week-old C57/BL/6 mice were killed using an intraperitoneal injection of phenobarbital (40 mg/kg). Eight mice were used for histological studies and three mice were used for RNA analysis. The tongue, earlobe, lungs, heart, stomach, small intestine, liver, spleen, kidney, and skeletal muscle of the mice were identified and either fixed in Carnoy's fixative and embedded in paraffin (five animals), or frozen in OCT (three animals). In three additional mice the tongue, earlobe, heart, lungs, small bowel, liver, spleen, and kidney were used for RNA extraction.

In order to compare mast cell distribution between mice and higher mammals, three normal adult mongrel dogs were killed after a rapid intravenous injection of KCl, and segments from the tongue, earlobe, lungs, heart, stomach, small bowel, liver, kidney, and skeletal muscle were fixed in Carnoy's fixative and embedded in paraffin.

Mast cell staining and quantitation

Histochemical staining with toluidine blue (Sigma, St. Louis, Mo., USA; Melinek and Mirolli 1992) and alcian blue/safranin staining (Valchanov and Proctor 1999) was performed in order to identify mast cells in normal murine tissues. For toluidine blue staining, slides were rinsed with PBS (Gibco BRL, Grand Island, N.Y., USA) for 10 min, stained with 0.5% w/v toluidine blue (Sigma) in 0.5 N HCl (Baker, Philipsburg, N.J., USA) for 30 min, and counterstained for 1 min with eosin (Harleco EM Science, Gibbstown, N.J., USA). Mast cells were easily identified by the ability of their granules to exhibit metachromatic staining. Histochemical staining with alcian blue/safranin was performed by incubating sections for 20 min with a staining solution prepared by mixing alcian blue (0.36%; Aldrich, Milwaukee, Wis., USA), safranin (0.012%), and ferric sulfate (0.48% w/v) (both from Sigma) in 0.2 M sodium acetate (VWR, Westchester, Pa., USA; pH=1.4). Subsequently slides were rinsed in deionized water, dehydrated in isobutanol for 2 min (Baker), cleared in xylenes for 1 min, and mounted.

Quantitative analysis of mast cell density in murine and canine organs was performed by counting the number of toluidine blue-positive mast cells in ten high power fields (400×). Mast cell density was expressed as cells/mm^2.

Detection of tryptase and chymase enzymatic activity in murine tissues

Tryptase amidolytic activity was detected in normal murine tissues as previously described (Valchanov and Proctor 1999). Frozen sections were fixed in absolute alcohol (Harleco EM Science) for 10 min at room temperature. Two different substrates were used with similar results: z-Ala-Ala-Lys-4-methoxy-2-naphthylamide (Z-AAK-mna) and z-Gly-Pro-Arg-4-methoxy-2-naphthylamide (Z-GPR-mna) (both from Enzyme System Products, Dublin, Calif., USA). Substrate stock solutions were prepared by dissolving the substrate in dimethylformamide (10 mg/ml; Sigma). Subsequently, the reaction mixture was prepared containing 0.25 mg/ml substrate diluted in Fast Garnet GBC (1 mg/ml in sodium acetate buffer, 0.1 M, pH=5.0; Sigma). Sections were incubated with the reaction mixture for 2 h at 37°C. Following incubation the sections were rinsed under deionized water for 1 min, and counterstained with methyl green (Sigma; 2% w/v chloroform extracted) dissolved in 0.1 M sodium acetate, pH 5.0, for 5 min. Subsequently, the methyl green solution was rinsed off the slides in deionized water (1 min) and the reaction was developed in an aqueous solution of cupric sulfate (10% w/v), magnesium sulfate (10% w/v), and potassium bicarbonate (2% w/v) (all from Sigma) for 5 min. The slides were then rinsed in deionized water (1 min) mounted using aqueous mounting media, and examined with a Zeiss Axioskop light microscope.

In order to demonstrate chymase amidolytic activity the naphthol-AS-D chloroacetate reaction was used. The following reagents were purchased: naphthol AS-D chloroacetate, pararosaniline, sodium nitrite, sodium barbitone, (all from Sigma), and aqueous HCl (2.0 N; Baker Analyzed). Solutions were prepared as follows: (a) naphthol AS-D chloroacetate solution in dimethylformamide (10 mg/ml), (b) pararosaniline solution in aqueous HCl (40 mg/ml), (c) sodium nitrite solution in deionized water (40 mg/ml), and (d) barbitone solution, 20 ml of a 2.9% w/v sodium barbitone solution containing 1.9% (w/v) sodium acetate was mixed with 16 ml of an aqueous 5% v/v HCl solution (2.0 N) in deionized water. Subsequently the pararosaniline solution was mixed with the sodium nitrite solution (40 mg/ml) in equal volumes. The barbitone solution was then adjusted to pH 6.13 with 2.0 N HCl. The pararosaniline solution (0.8 ml) was then mixed with the pH-adjusted barbitone solution (36 ml). The reaction mixture was prepared by adding 1 ml naphthol-AS-D chloroacetate solution. Frozen tissue sections were fixed with absolute ethanol for 30 min, incubated with the reaction mixture for 30 min, then rinsed in deionized water for 1 min. After counterstaining with hematoxylin (Harleco EM Science) the sections were rinsed in deionized water (1 min) then in acid ethanol (Sigma) for 1 min and in Scott's tap water (0.2% potassium bicarbonate, 2% magnesium sulfate in deionized water), mounted, and examined using a Zeiss Axioskop light microscope.

Immunohistochemistry

Sequential 3- to 5-µm sections from paraffin-embedded samples were cut by microtomy. Immunostaining with the rabbit antihistamine antibody (Research Diagnostics, Flanders, N.J., USA) and the macrophage-specific rat anti-mouse antibody F4/80 (Serotec, Oxford, UK; Hirsch et al. 1981) was performed using the ELITE rabbit and rat kit (Vector Laboratories, Burlingame, Calif., USA), respectively, as previously described (Frangogiannis et al. 1998, 2000). Briefly, sections were pretreated with a solution of 3% hydrogen peroxide (Sigma) to inhibit endogenous peroxidase activity and incubated with 2% horse serum to block non-specific protein binding. Subsequently, they were incubated with the primary antibody for 2 h at room temperature. After rinsing with PBS, the slides were incubated for 30 min with the secondary antibody. The slides were then rinsed with PBS and incubated for 30 min in ABC reagent (Hsu et al. 1981). Peroxidase activity was detected using diaminobenzidine (DAB) with nickel (Vector). Slides were counterstained with eosin. Sections incubated with non-immune serum were used as negative controls.

RNA extraction

All solutions for RNA analysis were treated with 0.1% diethylpyrocarbonate and sterilized or prepared in diethylpyrocarbonate-treated water. Total RNA was isolated from whole heart according to the acid-guanidinium-thiocyanate-phenol-chloroform method

(Chomczynski and Sacchi 1987). Briefly, whole hearts were homogenized in RNA STAT-60 solution (Tel-Test, Friendswood, Tex., USA). For RNA extraction, 0.2 vol R-chloroform were then added per volume homogenate. This mixture was incubated on ice for 15 min, and then spun at 12,000 *g* for 15 min at 4°C. The supernatant was transferred to another tube, and an equal volume of isopropanol was added for RNA precipitation overnight at 4°C. The tubes were then spun at 12,000 *g* for 15 min at 4°C, and the supernatant was then decanted. The pellet was washed twice with 75% ethanol, briefly dried, and dissolved in 0.1% diethylpyrocarbonate-treated water. Quantitation and purity of RNA were assessed by A^{260}/A^{280} UV absorption, and RNA samples with ratios above 1.9 were utilized for further analysis.

Ribonuclease protection assay and quantitation

The expression levels of SCF, M-CSF, and GM-CSF were determined using a ribonuclease protection assay (RPA). A commercially available kit (Riboquant kit; Pharmingen, San Diego, Calif., USA) and antisense RNA probe were utilized according to the manufacturer's protocol as previously described (Nossuli et al. 2001). Phosphorimaging of the RPA gels was performed with a Storm 860 phosphorimager (Molecular Dynamics, Calif., USA). Signals were quantified using Image QuaNT software and normalized to L32.

Results

Mast cell distribution in normal murine tissues

Toluidine blue staining was used to identify mast cells in normal tissues of C57/BL/6 mice and dogs. Mast cells were recognized as round, or elongated cells with metachromatic granular staining. Mast cells were abundant in the murine dermis (Fig. 1A). Many dermal mast cells exhibited long tail-like cytoplasmic projections (Fig. 1B) filled with granular content. The mouse tongue was particularly rich in mast cells with a smooth spherical shape, located throughout the submucosal region, adjacent to blood vessels and striated muscle (Fig. 1C). In the skeletal muscle a significant number of mast cells was noted in the perimysial and epimysial connective tissue, and in close proximity to vessels. Arteries demonstrated a significant number of mast cells, almost exclusively localized in the adventitia (Fig. 1D). Mast cells were extremely rare in the mouse lung parenchyma (Fig. 1E), but were commonly found around the bronchi. Few mast cells were found in the murine heart (Fig. 1G), most located in the epicardial side. The gastric wall contained a significant number of mucosal and submucosal mast cells. Occasional mast cells were found in the small bowel submucosa (Fig. 1I). Mast cells were extremely rare in the intestinal villi (Fig. 1I). Practically no mast cells were noted in the hepatic parenchyma (Fig. 1K). Occasional mast cells were noted in the murine kidney (most located in the renal capsule) and spleen (predominantly found in the red pulp or the perifollicular zone). Comparison of the mast cell distribution between mice and dogs showed some striking differences. In contrast to mice, normal dogs exhibited a high mast cell density in the lung (Fig. 1F; Table 1), small bowel mucosa and submucosa (Fig. 1J), and liver (Fig. 1L). However, the canine spleen and kidney demonstrated only rare mast cells, like their murine homologues (Table 1).

Phenotypic characteristics of murine mast cells

Alcian blue/safranin staining identified connective tissue type mast cells in murine tissues. Dermal (Fig. 2A), tongue, skeletal muscle (Fig. 2B), and cardiac mast cells showed positive staining for safranin. In the murine stomach, mucosal alcian blue-positive safranin-negative mast cells (Fig. 2C) and submucosal safranin-positive connective tissue-type mast cells were noted (Fig. 2D). In the murine bowel we found very few safranin-positive submucosal mast cells. Mucosal bowel mast cells could not be specifically identified with this method due to the intense alcian blue staining of intestinal goblet cells. In contrast, goblet cells in the mouse lung demonstrated much weaker alcian blue staining.

Immunohistochemical staining demonstrated intense histamine immunoreactivity in murine mast cells (Fig. 3). We also examined expression of tryptase and chymase enzymatic activity in murine mast cells using established histochemical techniques. We localized tryptase activity in connective tissue mast cells in the murine

Table 1 Comparison of the mast cell density (cells/mm^2) in various anatomical sites of C57/BL/6 mice, dogs, rats (Tsai et al. 1991), and WCB6F1- +/+ mice (Ando et al. 1993). (*M* Mucosa, *S* submucosa, *NR* not reported)

Anatomical site	C57/BL/6 mouse	Dog	WCB6F1- +/+ mouse	Rat
Liver	0	45.4±18	0	3.6±0.4
Kidney	0.19±0.03	0.03±0.03	NR	NR
Spleen	0.58±0.09	0.7±0.3	1±0.2	0.07±0.02
Skeletal muscle	13.1±2.1	3.5±1.3	NR	NR
Tongue	14.5±2.6	23.8±4	NR	NR
Heart (LV)	0.6±0.2	6.8±1.6	0.7±0.1	NR
Skin (dermis)	135±16.7	24.5±1.9	275±11	26±3
Stomach	M: 14.4±4.2	M: 332±40.9	M: 27±5	M: 12±3
	S: 12.2+5.5	S: 65.8+12.1	S: 140±18	S: 45±8
Small bowel	M: 1.3±0.9	M: 154.5±42.1	NR	M: 38±12
	S: 1.7±0.5	S: 93+37.8		S: 19±4
Lung	0.09±0.07	62.2±28.5	0	7±0.4

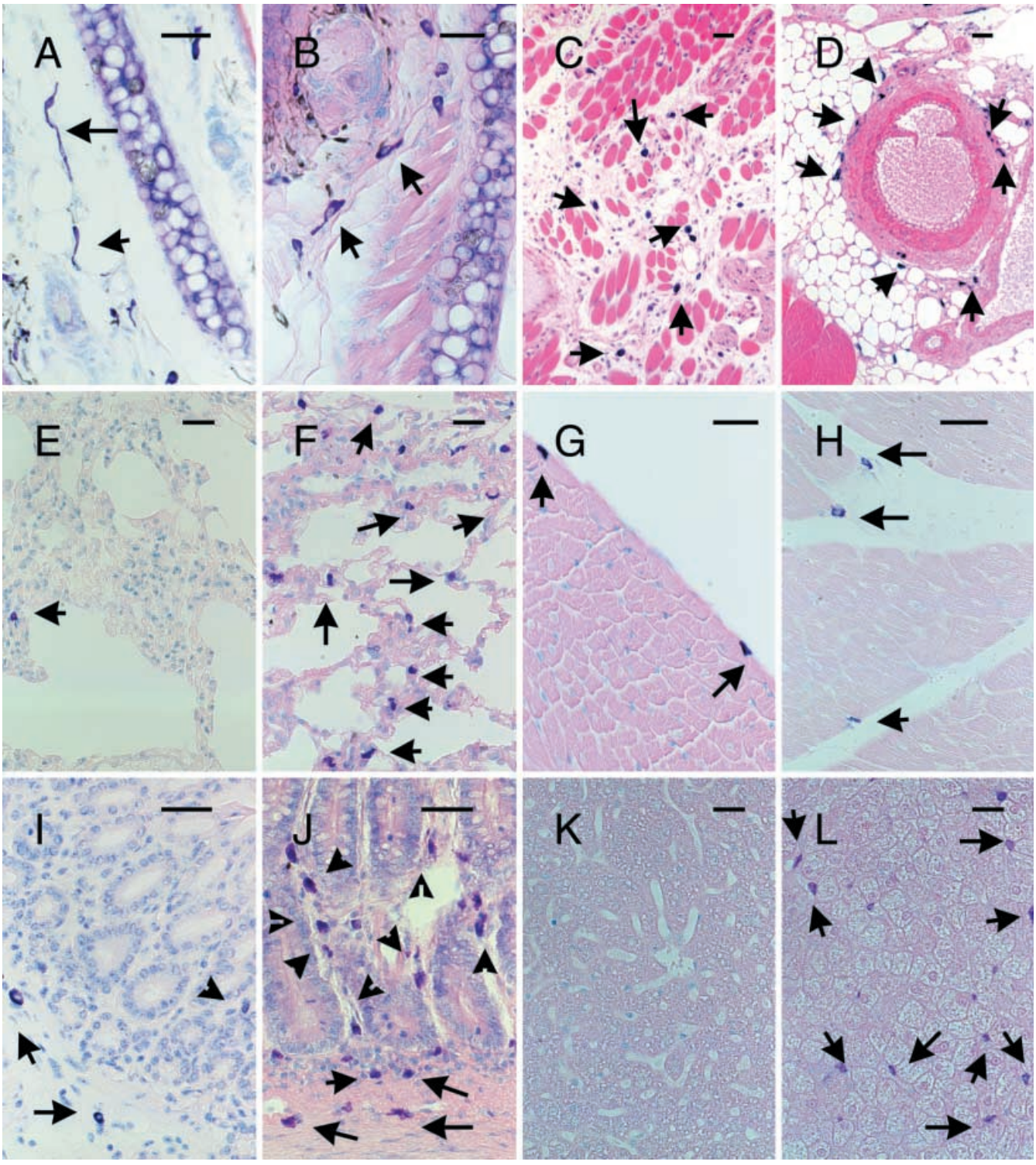

Fig. 1A–L Toluidine blue staining identifies mast cells in normal murine and canine tissues. **A**, **B** Abundant mast cells were noted in the murine dermis. Some of these mast cells exhibited long cytoplasmic projections (*arrows*) filled with granular material. **C** The tongue contained many round densely granulated mast cells (*arrows*). **D** Arterial trunks demonstrated a significant number of mast cells (*arrows*), almost exclusively located in the adventitia. **E** Very few mast cells (*arrow*) were noted in the murine pulmonary parenchyma. **F** In contrast, the canine lung demonstrated a significant number of mast cells (*arrows*). **G** Occasional mast cells were found in the murine heart (*arrows*). **H** Canine cardiac mast cells were more numerous and usually found around vessels. **I** The murine bowel contained a small number of mast cells in the submucosa (*arrows*) and the mucosa (*arrowhead*). **J** The canine bowel had a large number of mucosal (*arrowheads*) and submucosal (*arrows*) mast cells. **K** Mast cells were very rarely found in the mouse liver. **L** In contrast, abundant mast cells were found in the canine liver (*arrows*). *Scale bar* 25 µm

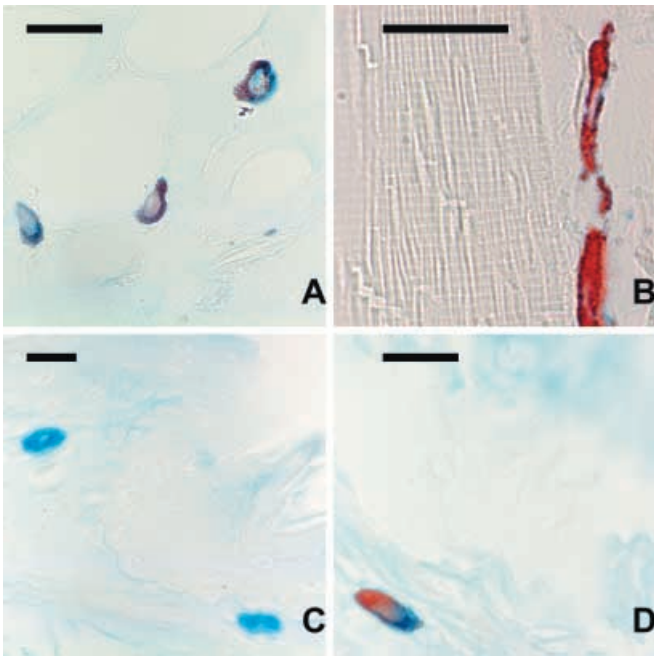

Fig. 2A–D Mast cell staining with alcian blue/safranin. **A** Dermal mast cells showed many safranin-positive granules. **B** Skeletal muscle mast cells were strongly positive for safranin. **C** In the gastric mucosa relatively few safranin-negative mast cells were found. **D** In contrast, submucosal gastric mast cells were safranin positive. *Scale bar* 15 µm

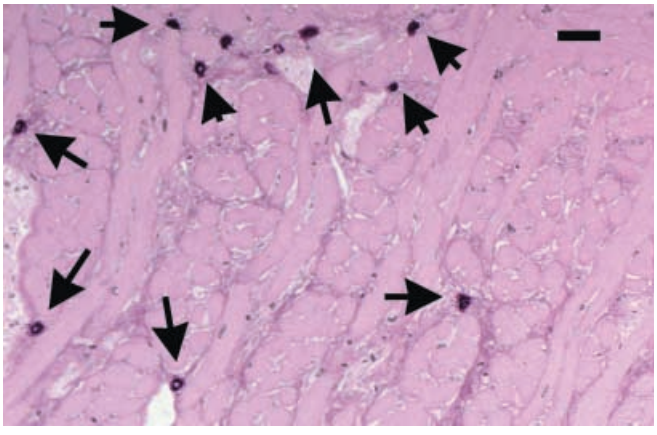

Fig. 3 Murine mast cells demonstrate intense immunoreactivity for histamine. Peroxidase-based immunostaining with antihistamine antibody identifies mast cells in the murine tongue (*arrows*). *Scale bar* 25 µm

tongue (Fig. 4A) and skin (Fig. 4B). Furthermore, naphthol AS-D chloroacetate staining indicated the presence of chymase enzymatic activity in the cytoplasmic granules of mast cells in all organs examined. Figure 5 demonstrates chymase-expressing mast cells in the mouse tongue (Fig. 5A), earlobe (Fig. 5B), bowel (Fig. 5C), and spleen (Fig. 5D).

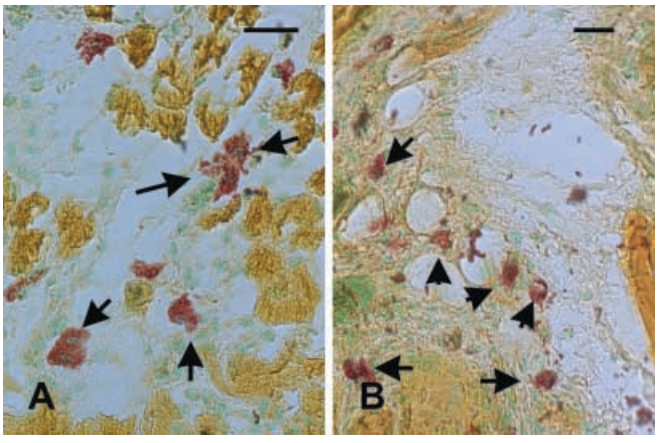

Fig. 4A, B Murine mast cells show tryptase enzymatic activity. Mast cells (*arrows*) in the murine tongue (**A**) and dermis (**B**) are identified using an enzymatic technique for tryptase. *Scale bar* 20 µm

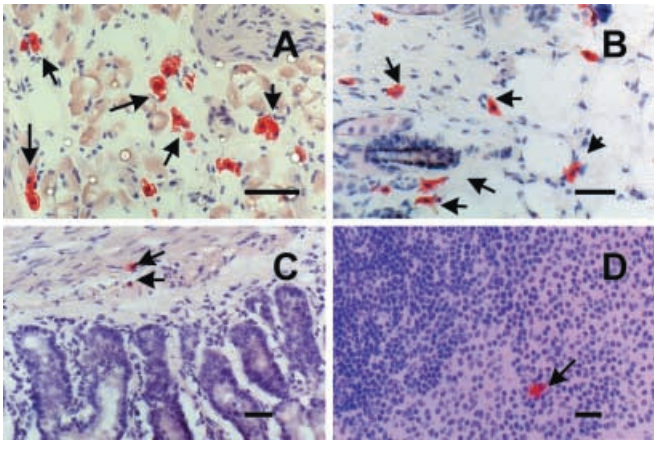

Fig. 5A–D Murine mast cells show chymase enzymatic activity. Abundant mast cells in the tongue (**A**) and dermis (**B**) are identified using naphthol AS-D chloroacetate staining. **C** Few mast cells were identified in the bowel submucosa (*arrows*). **D** The spleen showed occasional mast cells predominantly located in the red pulp (*arrow*). *Scale bar* 20 µm

Macrophages in control murine tissues

Staining with the monoclonal antibody F4/80 identified resident macrophages in murine organs as previously described (Hume and Gordon 1983; Hume et al. 1983). The splenic red pulp was rich in F4/80-positive cells (Fig. 6A). The lung parenchyma was filled with alveolar macrophages (Fig. 6C), whereas only few F4/80-positive cells were found in the heart. The liver contained a large population of macrophages (Fig. 6B). The bowel showed high numbers of macrophages in the lamina propria and the submucosa (Fig. 6D). Significant numbers of macrophages were noted in the skeletal muscle and the kidney (data not shown). In contrast, macrophages were less commonly found in the tongue and the earlobe, where large mast cell populations have been identified.

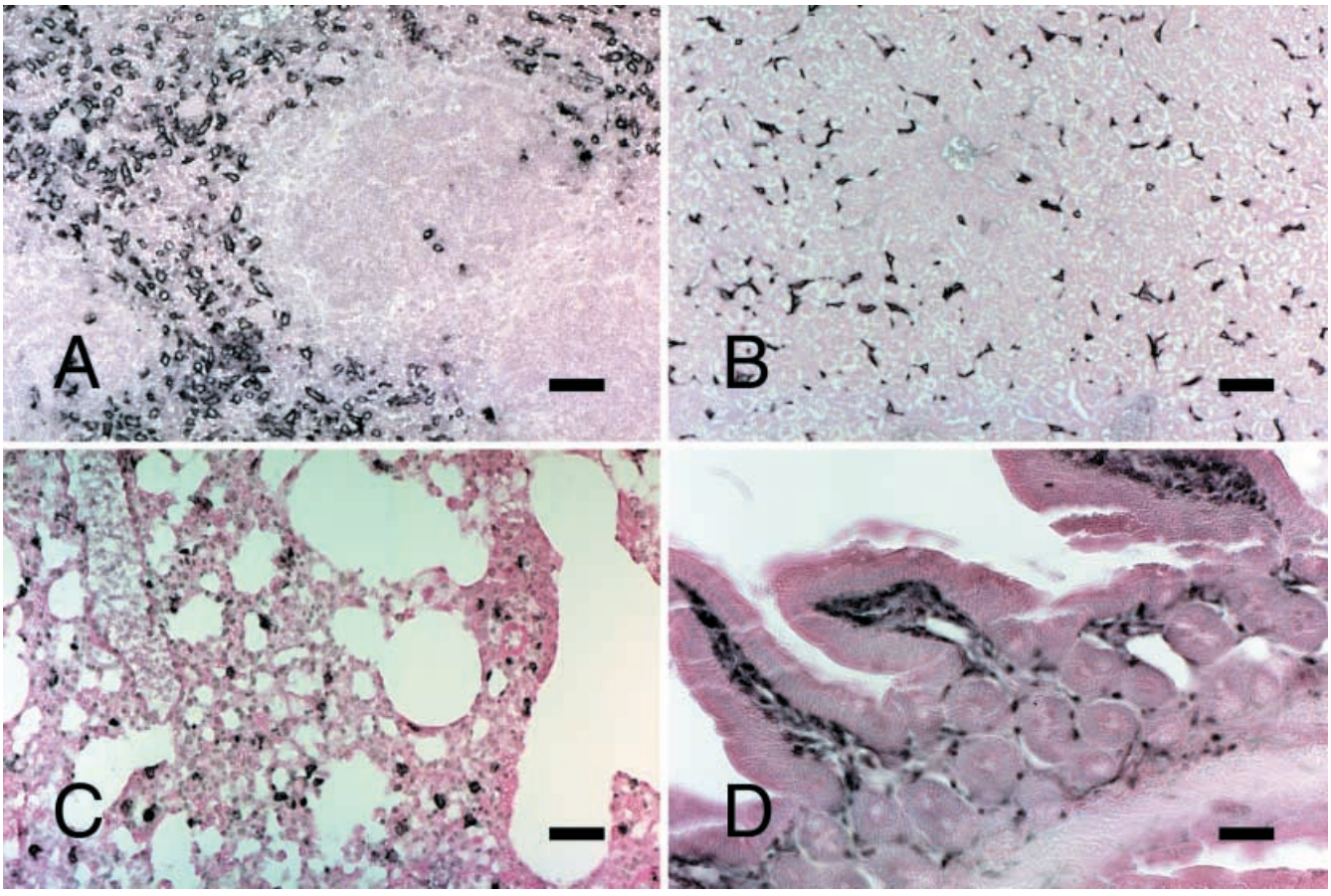

Fig. 6A–D Identification of murine macrophages using the antibody F4/80. **A** Macrophage staining in the murine spleen. **B** Hepatic macrophages stained with F4/80. **C** Alveolar macrophages. **D** Macrophages in the murine bowel are predominantly localized in the lamina propria and the submucosa. *Scale bar* 50 µm

Expression of SCF, M-CSF, and GM-CSF mRNA in normal murine tissues

Utilizing a nuclease protection assay we examined constitutive expression of SCF mRNA in normal murine tissues (Figs. 7, 8A). High SCF mRNA synthesis was noted in the lung, with lower levels in the spleen, bowel, heart, and tongue. Macrophage CSF mRNA expression was found in all tissues examined and was especially high in the lung, spleen, heart, and tongue (Figs. 7, 8B). High-level constitutive expression of GM-SCF mRNA was noted in the lung. In contrast the normal murine heart contained negligible amounts of GM-CSF mRNA (Figs. 7, 8C).

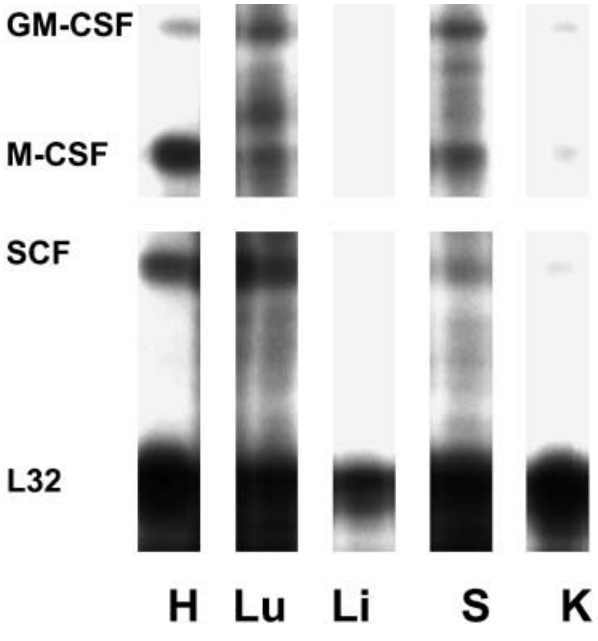

Fig. 7 Nuclease protection assay shows constitutive growth factor mRNA expression in mouse tissues. Note that the normal mouse heart shows significant expression of macrophage colony stimulating factor (*M-CSF*) and stem cell factor (*SCF*) mRNA but negligible granulocyte macrophage colony stimulating factor (*GM-CSF*) mRNA synthesis. In contrast, the lung demonstrates high constitutive mRNA levels for all three growth factors. *H* Heart, *Lu* lung, *Li* liver, *S* spleen, *K* kidney

Discussion

Mast cells in normal tissues

When Enerback recognized distinct mast cell subpopulations in the rat based on fixation-dependent histochemical staining characteristics (Enerback 1966), the substantial

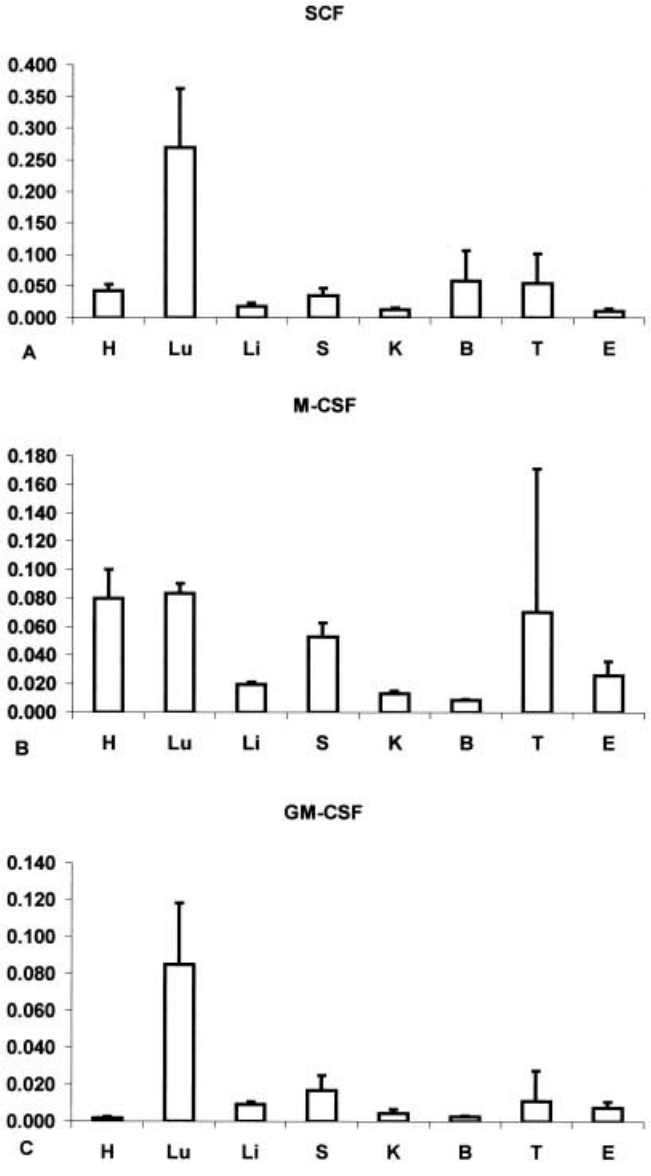

Fig. 8 Quantitative analysis of SCF (**A**), M-CSF (**B**), and GM-CSF (**C**) mRNA expression in normal mouse tissues. *H* Heart, *Lu* lung, *Li* liver, *S* spleen, *K* kidney, *B* bowel, *T* tongue, *E* earlobe

heterogeneity of mast cells became evident. More recently, differences in protease expression within anatomically distinct mast cell populations were recognized (Stevens et al. 1994; Friend et al. 1996; May 1999). Rodent mast cells were identified as connective tissue-type mast cells or mucosal-type mast cells. We present a detailed description of the distribution and the morphological characteristics of mast cells in control tissues from C57/BL/6 mice, a strain commonly used for investigations of the inflammatory response (Nossuli et al. 2001), and compare mast cell density in mouse organs with other mammalian species (Table 1). Large numbers of mast cells were found in the murine tongue and dermis as previously described (Majeed 1994). Dermal mast cells often exhibited long cytoplasmic projections, a feature recently identified in dendritic mast cells described in the human nasal mucosa (Jacobi et al. 1998). In contrast, mast cells in other murine organs were round or elongated granular cells without cytoplasmic projections, suggesting that mouse mast cells demonstrate significant heterogeneity with respect to their morphological features.

Murine parenchymal organs showed relatively low numbers of mast cells. The mouse lung had practically no alveolar mast cells. In contrast, significant numbers of mast cells were found in close proximity to the bronchial smooth muscle, supporting the potential role of mast cell mediators in regulating airway reactivity. Rare mast cells were found in the murine heart, predominantly localized in the epicardial half of the myocardium. Numerous mast cells were noted in the murine skeletal muscle, predominantly located in the endomysial and perimysial connective tissue. Vascular trunks were also commonly associated with a large number of adventitial mast cells. Mast cells were rarely found in the spleen and kidney, whereas they were practically absent in the murine liver. A significant mast cell population was found in the mouse stomach and a much smaller one in the intestine (Table 1). Mucosal mast cells were rarely found in the normal murine gut, which is consistent with previously reported findings (Ruitenberg and Elgersma 1976; Friend et al. 1996). In contrast, helminth-infected rodents show a pronounced increase in the number of intestinal mucosal mast cells (Miller and Jarrett 1971; Friend et al. 1996, 1998; Scudamore et al. 1997), exhibiting a reactive phenomenon related to the expression of T-cell-derived cytokines and leads to a greater than 25-fold increase in mast cell density throughout the villi.

Mast cell distribution in various anatomical sites of C57/BL/6 mice was quite similar to the mast cell content reported in WCB6F1- +/+ mice (Ando et al. 1993), the wild-type littermates of mast cell-deficient mice (Table 1). However, comparison with the mast cell distribution in other mammals revealed striking differences: in contrast to mice, dogs have significant mast cell populations in the bowel (Fig. 1J), lungs (Fig. 1F), and liver (Fig. 1L). In addition, normal rats show significant numbers of mast cells in the bowel mucosa and submucosa (Tsai et al. 1991; Table 1). These findings show significant species-specific differences in mast cell distribution and density in various anatomical sites, suggesting caution in extrapolating findings derived from experiments in mice to higher mammals.

Mast cell protease expression

Tryptase and chymase are synthesized in large quantities by mast cells and appear to participate in a variety of inflammatory processes (Caughey 1989; Welle 1997; Coussens et al. 1999). Murine mast cells exhibit chymase and tryptase enzymatic activity in the tongue, earlobe, and stomach (Wolters et al. 2001). Which chymase a mast cell expresses in the BALB/c mouse seems to be dictated by both the current and previous microenvironments of the cell (Friend et al. 1996, 1998; Xia et al. 1996). Friend and colleagues recently reported that the mast cells in the jeju-

num of *Trichinella spiralis*-infected BALB/c mice undergo time- and strata-dependent changes in their expression of the three chymases mMCP-1, mMCP-2, and mMCP-5 (Friend et al. 1996). In addition, strain-specific differences in protease expression by murine mast cells have been reported (Ghildyal et al. 1994), and may reflect intrinsic abnormalities of the mast cell-committed precursors. Our experiments demonstrated the presence of chymase and tryptase enzymatic activity in connective tissue-type mast cells located in the murine tongue, earlobe, spleen, and bowel. Recently Valchanov and colleagues reported the presence of mast cells with tryptase activity in the gastric but not the intestinal mucosa of adult C3H, WHT, and C3A mice (Valchanov and Proctor 1999). Mucosal mast cells were extremely rare in the intestine from normal C57/BL/6 mice, thus, we were unable to assess their protease content.

Distribution of macrophages in murine organs

The monoclonal antibody F4/80 specifically identified murine macrophages, as previously described (Hume and Gordon 1983; Hume et al. 1983). As expected a large population of F4/80+ cells was found in the splenic red pulp. Macrophages in the liver, lung, bowel, and kidney were also identified and were much more numerous than mast cells in the same anatomical locations. In contrast, macrophages were less numerous than mast cells in the tongue and earlobe.

Constitutive expression of SCF, M-CSF, and GM-CSF in normal murine tissues

Support of mast cell and macrophage growth in normal tissues requires the constitutive expression of specific growth factors, crucial for their survival and growth. Stem cell factor (Galli et al. 1994), also termed c-kit ligand, is a pleiotropic growth factor involved in the early stages of hematopoiesis, which is important for mast cell chemotaxis (Meininger et al. 1992), differentiation, and survival (Iemura et al. 1994; Galli et al. 1995). Macrophage-CSF and GM-CSF (Wiktor-Jedrzejczak and Gordon 1996) are critical for macrophage growth and survival. We examined the constitutive expression of SCF, M-CSF, and GM-CSF in normal murine tissues, where they may create the microenvironment necessary to support mast cell and macrophage survival. Surprisingly, SCF was highly expressed in the lungs. Relatively low levels of constitutive SCF mRNA expression were found in other organs examined, suggesting that even in tissues with a high mast cell content (such as the earlobe and the tongue), low-level SCF mRNA synthesis is sufficient to support mast cell survival.

Our experiments also examined constitutive expression of M-CSF and GM-CSF mRNA in normal mouse tissues. High levels of M-CSF mRNA expression were found in the murine lung, heart, spleen, and tongue. This is consistent with previous studies (Troutt and Lee 1989; Roth et al. 1997) demonstrating constitutive levels of M-CSF expression in the lung, spleen, and heart with lower levels in the kidney and intestine. Our experiments clearly demonstrate that relatively small amounts of M-CSF mRNA synthesis are sufficient to support the large macrophage populations found in the liver and intestine. In addition, tissues with a relatively low macrophage content such as the heart, show significant constitutive expression of M-CSF. In the murine lung GM-CSF expression was particularly high, confirming previous experiments (Troutt and Lee 1989). In addition, the murine heart, an organ with relatively high M-CSF expression, exhibited negligible amounts of constitutive GM-CSF mRNA synthesis. Colony-stimulating factors (Sieff et al. 1988) and SCF (Heinrich et al. 1993) are constitutively expressed by a variety of cell types and may have an important role in regulating the distribution and function of the monocyte/macrophage and the mast cell system.

Acknowledgements The authors wish to thank Alida Evans and Stephanie Butcher for technical assistance, and Sharon Malinowski and Concepcion Mata for their editorial assistance with the manuscript. This work was supported by NIH grant HL-42550, the DeBakey Heart Center, and a grant from the Methodist Hospital Foundation (N.G.F.). Dr. Dewald is supported by the Deutsche Forschungsgemeinschaft.

References

Ando A, Martin TR, Galli SJ (1993) Effects of chronic treatment with the c-kit ligand, stem cell factor, on immunoglobulin E-dependent anaphylaxis in mice. Genetically mast cell-deficient Sl/Sld mice acquire anaphylactic responsiveness, but the congenic normal mice do not exhibit augmented responses. J Clin Invest 92:1639–1649

Borisov AB (1999) Regeneration of skeletal and cardiac muscle in mammals: do nonprimate models resemble human pathology? Wound Repair Regen 7:26–35

Caughey GH (1989) Roles of mast cell tryptase and chymase in airway function. Am J Physiol 257:L39–L46

Chomczynski P, Sacchi N (1987) Single-step method of RNA isolation by acid guanidinium thiocyanate-phenol-chloroform extraction. Anal Biochem 162:156–159

Coussens LM, Raymond WW, Bergers G, Laig-Webster M, Behrendtsen O, Werb Z, Caughey GH, Hanahan D (1999) Inflammatory mast cells up-regulate angiogenesis during squamous epithelial carcinogenesis. Genes Dev 13:1382–1397

Enerback L (1966) Mast cells in rat gastrointestinal mucosa: effects of fixation. Acta Pathol Microbiol Scand 66:289–302

Frangogiannis NG, Perrard JL, Mendoza LH, Burns AR, Lindsey ML, Ballantyne CM, Michael LH, Smith CW, Entman ML (1998) Stem cell factor induction is associated with mast cell accumulation after canine myocardial ischemia and reperfusion. Circulation 98:687–698

Frangogiannis NG, Burns AR, Michael LH, Entman ML (1999) Histochemical and morphological characteristics of canine cardiac mast cells. Histochem J 31:221–229

Frangogiannis NG, Mendoza LH, Lindsey ML, Ballantyne CM, Michael LH, Smith CW, Entman ML (2000) IL-10 is induced in the reperfused myocardium and may modulate the reaction to injury. J Immunol 165:2798–2808

Friend DS, Ghildyal N, Austen KF, Gurish MF, Matsumoto R, Stevens RL (1996) Mast cells that reside at different locations in the jejunum of mice infected with *Trichinella spiralis* exhibit sequential changes in their granule ultrastructure and chymase phenotype. J Cell Biol 135:279–290

Friend DS, Ghildyal N, Gurish MF, Hunt J, Hu X, Austen KF, Stevens RL (1998) Reversible expression of tryptases and chymases in the jejunal mast cells of mice infected with *Trichinella spiralis*. J Immunol 160:5537–5545

Fritz RB, Zhao ML (2001) Regulation of experimental autoimmune encephalomyelitis in the C57BL/6 J mouse by NK1.1+, DX5+, alpha beta+ T cells. J Immunol 166:4209–4215

Galli SJ, Tsai M, Wershil BK (1993) The c-kit receptor, stem cell factor, and mast cells. What each is teaching us about the others. Am J Pathol 142:965–974

Galli SJ, Zsebo KM, Geissler EN (1994) The kit ligand, stem cell factor. Adv Immunol 22:1–96

Galli SJ, Tsai M, Wershil BK, Tam SY, Costa JJ (1995) Regulation of mouse and human mast cell development, survival and function by stem cell factor, the ligand for the c-kit receptor. Int Arch Allergy Immunol 107:51–53

Ghildyal N, Friend DS, Freelund R, Austen KF, McNeil HP, Schiller V, Stevens RL (1994) Lack of expression of the tryptase mouse mast cell protease 7 in mast cells of the C57BL/6 J mouse. J Immunol 153:2624–2630

Gordon JR, Galli SJ (1990) Mast cells as a source of both preformed and immunologically inducible TNF-α/cachectin. Nature 346:274–276

Gordon JR, Burd PR, Galli SJ (1990) Mast cells as a source of multifunctional cytokines. Immunol Today 11:458–464

Gu L, Tseng S, Horner RM, Tam C, Loda M, Rollins BJ (2000) Control of TH2 polarization by the chemokine monocyte chemoattractant protein-1. Nature 404:407–411

Heinrich MC, Dooley DC, Freed AC, Band L, Hoatlin ME, Keeble WW, Peters ST, Silvey KV, Ey FS, Kabat D (1993) Constitutive expression of steel factor gene by human stromal cells. Blood 82:771–783

Hirsch S, Austyn JM, Gordon S (1981) Expression of the macrophage-specific antigen F4/80 during differentiation of mouse bone marrow cells in culture. J Exp Med 154:713–725

Hsu SM, Raine L, Fanger H (1981) Use of avidin-biotin-peroxidase complex (ABC) in immunoperoxidase techniques: a comparison between ABC and unlabeled antibody (PAP) procedures. J Histochem Cytochem 29:577–580

Hume DA, Gordon S (1983) Mononuclear phagocyte system of the mouse defined by immunohistochemical localization of antigen F4/80. Identification of resident macrophages in renal medullary and cortical interstitium and the juxtaglomerular complex. J Exp Med 157:1704–1709

Hume DA, Robinson AP, MacPherson GG, Gordon S (1983) The mononuclear phagocyte system of the mouse defined by immunohistochemical localization of antigen F4/80. Relationship between macrophages, Langerhans cells, reticular cells, and dendritic cells in lymphoid and hematopoietic organs. J Exp Med 158:1522–1536

Iemura A, Tsai M, Ando A, Weshil BK, Galli SJ (1994) The c-kit ligand, stem cell factor, promotes mast cell survival by suppressing apoptosis. Am J Pathol 144:321–328

Jacobi HH, Liang Y, Tingsgaard PK, Larsen PL, Poulsen LK, Skov PS, Haak-Frendscho M, Niles AL, Johansson O (1998) Dendritic mast cells in the human nasal mucosa. Lab Invest 78:1179–1184

Kahn DA, Archer DC, Gold DP, Kelly CJ (2001) Adjuvant immunotherapy is dependent on inducible nitric oxide synthase. J Exp Med 193:1261–1268

Kanwar S, Hickey MJ, Kubes P (1998) Postischemic inflammation: a role for mast cells in intestine but not in skeletal muscle. Am J Physiol 275:G212–G218

Kube P, Audige L, Kuther K, Welle M (1998) Distribution, density and heterogeneity of canine mast cells and influence of fixation techniques. Histochem Cell Biol 110:129–135

Kupper TS (1996) The utility of transgenic mouse models in the study of cutaneous immunology and inflammation. J Dermatol 23:741–745

Majeed SK (1994) Mast cell distribution in mice. Arzneimittelforschung 44:1170–1173

May CA (1999) Mast cell heterogeneity in the human uvea. Histochem Cell Biol 112:381–386

Meininger CJ, Yano H, Rottapel R, Bernstein A, Zsebo KM, Zetter BR (1992) The c-kit receptor ligand functions as a mast cell chemoattractant. Blood 79:958–963

Melinek R, Mirolli M (1992) Histochemical study of the heart of the axolotl (*Ambystoma mexicanum*). Anat Rec 233:13–17

Miller HR, Jarrett WF (1971) Immune reactions in mucous membranes. I. Intestinal mast cell response during helminth expulsion in the rat. Immunology 20:277–288

Nossuli TO, Frangogiannis NG, Knuefermann P, Lakshminarayanan V, Dewald O, Evans AJ, Peschon J, Mann DL, Michael LH, Entman ML (2001) Brief murine myocardial I/R induces chemokines in a TNF-alpha-independent manner: role of oxygen radicals. Am J Physiol Heart Circ Physiol 281:H2549–H2558

Rohan RM, Fernandez A, Udagawa T, Yuan J, D'Amato RJ (2000) Genetic heterogeneity of angiogenesis in mice. FASEB J 14:871–876

Roth P, Bartocci A, Stanley ER (1997) Lipopolysaccharide induces synthesis of mouse colony-stimulating factor-1 in vivo. J Immunol 158:3874–3880

Ruitenberg EJ, Elgersma A (1976) Absence of intestinal mast cell response in congenitally athymic mice during *Trichinella spiralis* infection. Nature 264:258–260

Scudamore CL, McMillan L, Thornton EM, Wright SH, Newlands GF, Miller HR (1997) Mast cell heterogeneity in the gastrointestinal tract: variable expression of mouse mast cell protease-1 (mMCP-1) in intraepithelial mucosal mast cells in nematode-infected and normal BALB/c mice. Am J Pathol 150:1661–1672

Shapiro SD (1997) Mighty mice: transgenic technology "knocks out" questions of matrix metalloproteinase function. Matrix Biol 15:527–533

Sieff CA, Niemeyer CM, Mentzer SJ, Faller DV (1988) Interleukin-1, tumor necrosis factor, and the production of colony-stimulating factors by cultured mesenchymal cells. Blood 72:1316–1323

Smith MA, Pallister CJ, Smith JG (2001) Stem cell factor: biology and relevance to clinical practice. Acta Haematol 105:143–150

Stevens RL, Friend DS, McNeil HP, Schiller V, Ghildyal N, Austen KF (1994) Strain-specific and tissue-specific expression of mouse mast cell secretory granule proteases. Proc Natl Acad Sci U S A 91:128–132

Troutt AB, Lee F (1989) Tissue distribution of murine hemopoietic growth factor mRNA production. J Cell Physiol 138:38–44

Tsai M, Shih LS, Newlands GF, Takeishi T, Langley KE, Zsebo KM, Miller HR, Geissler EN, Galli SJ (1991) The rat c-kit ligand, stem cell factor, induces the development of connective tissue-type and mucosal mast cells in vivo. Analysis by anatomical distribution, histochemistry, and protease phenotype. J Exp Med 174:125–131

Valchanov KP, Proctor GB (1999) Enzyme histochemistry of tryptase in stomach mucosal mast cells of the mouse. J Histochem Cytochem 47:617–622

Walsh LJ, Trinchieri G, Waldorf HA, Whitaker D, Murphy GF (1991) Human dermal mast cells contain and release tumor necrosis factor alpha, which induces endothelial leukocyte adhesion molecule 1. Proc Natl Acad Sci U S A 88:4220–4224

Weindruch R, Masoro EJ (1991) Concerns about rodent models for aging research. J Gerontol 46:B87–B88

Welle M (1997) Development, significance, and heterogeneity of mast cells with particular regard to the mast cell-specific proteases chymase and tryptase. J Leukoc Biol 61:233–245

Wiktor-Jedrzejczak W, Gordon S (1996) Cytokine regulation of the macrophage (M phi) system studied using the colony stimulating factor-1-deficient op/op mouse. Physiol Rev 76:927–947

Wolters PJ, Pham CT, Muilenburg DJ, Ley TJ, Caughey GH (2001) Dipeptidyl peptidase I is essential for activation of mast cell chymases, but not tryptases, in mice. J Biol Chem 276:18551–18556

Xia Z, Ghildyal N, Austen KF, Stevens RL (1996) Post-transcriptional regulation of chymase expression in mast cells. A cytokine-dependent mechanism for controlling the expression of granule neutral proteases of hematopoietic cells. J Biol Chem 271:8747–8753